Electrophosphorescent Chelating Copolymers Based on Linkage Isomers of Naphthylpyridine−Iridium Complexes with Fluorene

Hongyu Zhen,[†] Chan Luo,[†] Wei Yang,*[,†] Wuyuan Song,[‡] Bin Du,[†] Jiaxing Jiang,[†] Changyun Jiang,[†] Yong Zhang,[†] and Yong Cao[†]

Institute of Polymer Optoelectronic Materials and Devices, Key Laboratory of Specially Functional Materials and Advanced Manufacturing Technology, South China University of Technology, Guangzhou 510640, China, and Inspection Center on Chemicals, Minerals & Metallic Materials, Guangzhou Entry-Exit Inspection & Quarantine Bureau of China, Guangzhou, China

Received September 21, 2005; Revised Manuscript Received January 10, 2006

ABSTRACT: A series of phosphorescent chelating copolymers based on the linkage isomers of 2-(1-naphthalene)-pyridine− and 2-(2-naphthalene)pyridine−bicycloiridium complexes were synthesized by Suzuki polycondensation of A−A- and B−B-type monomers. These linkage isomers-based copolymers show distinct differences in their photophysical and electroluminescence properties. The phosphorescent emission band of the copolymer PF1−NpyIrm is in the region of 630 nm, whereas copolymers PF2−NpyIrm show an emission with the peak maximum at 590 nm, which are both red-shifted around 20 nm compared with the emissions of the pristine complexes. The highly efficient saturated red-phosphorescent PLEDs were achieved on the basis of copolymers PF1−NpyIrm. The best device performances are observed from copolymer PF1−NpyIrm1 with an external quantum efficiency (η_{ext}) of 6.5% photon/electron (ph/el) at the current density of 38 mA/cm^2, with the emission peak at 630 nm ($x = 0.65$, $y = 0.31$) and the luminance of 926 cd/m^2. The efficiency remains as high as $\eta_{ext} = 5.3\%$ ph/el at a high current density of 100 mA/cm^2. No remarkable efficiency decay with the increase in current density shows that the chelating copolymers are promising candidate materials for phosphorescent polymer light-emitting diodes (PHPLEDs).

Introduction

Electrophosphorescent polymers containing heavy-metal complexes have been attracting much attention because of their high quantum efficiency.[1] Unlike electrofluorescence, electrophosphorescence can make use of both singlet and triplet excitons owing to strong spin−orbital coupling of heavy-metal ions in phosphorescent complexes, thereby theoretically achieving 100% of internal quantum efficiency.[1b] There are many reports focused on electrophosphorescent polymers based on Ir complexes due to the relatively short phosphorescent lifetime and high luminous efficiency.[2] Lee et al.[3] synthesized the nonconjugated polyethylene main chain with phenylpyridine attached to side chain as a ligand and pendant *N*-vinylcarbazole as host materials. A high external quantum efficiency of 4.4% ph/el was achieved at a current density of 6.4 mA/cm^2. A similar approach of using nonconjugated main chain with pendant diketone was reported by Tokito et al.[4] High external quantum efficiencies of 5.5%, 9%, and 3.5% in red, green, and blue PLEDs were respectively achieved. The phosphorescent conjugated polymers based on polyfluorene backbone with diketone pendant attached to the 9-carbon position of fluorene were reported by Chen et al.[5] The device from the graft polymer of 1.3 mol % iridium(III) bis(2-(2′-benzo-[4,5-α]thienyl)pyridinato-*N*,*C*$^{3'}$)acetylacetonate complex [(btp)$_2$Ir(acac)] with diketone attached to the 9-position of fluorene ring has shown an external quantum efficiency of 1.59% ph/el and a power efficiency of 2.8 cd/A at 7.0 V with the luminance of 65 cd/m^2 and the peak emission at 610 nm. The device of the fluorene-*alt*-carbazole copolymers grafted in the N-position with 1-phenylisoquinoline−Ir complex shows the highest external quantum efficiency of 4.9% ph/el and the luminous efficiency of 4.0 cd/A with 240 cd/m^2 at a bias voltage of 7.7 V and a peak emission of 610 nm.[6]

Recently, the conjugated chelating phosphorescent polymers that possess M−C σ or π bonds in the backbone have attracted substantial attention. A series of conjugated well-defined oligo- and polyfluorenyl bis-cyclometalated Ir complexes were synthesized with Suzuki homo-polycondensation of A−B-type monomer by Sandee et al.[7] The maximum external quantum efficiencies of 1.5% and 0.12% ph/el were obtained respectively by introducing (btp)$_2$Ir(acac) and (ppy)$_2$Ir(acac) complexes covalently into the poly(9,9′-dioctylfluorene) backbone. In our previous work, iridium(III) bis(2-*p*-tolylpyridine-*C*$^{2'}$,*N*)-2,2,6,6-tetramethyl-3,5-heptanedione [(mppy)$_2$Ir(hmacac)] as a repeat unit was introduced into the backbone of fluorene-*alt*-carbazole (PFCz) copolymer, and a maximal external quantum efficiency of 4.6% ph/el at the maximal wavelength of 577 nm was achieved.[8] In this case, the conjugated segments play both roles: a part of the ligand and a host for the energy transfer system. The high-efficiency energy transfer from the polymer host to the triplet metal complex in polymer main chain via an efficient intramolecular energy transfer would be expected.[9] Although considerable studies have focused on phosphorescent iridium complexes, little is known about their linkage isomers and their corresponding photophysical and electroluminescence properties;[10] even less is known about the chelating polymers based on the linkage isomer complexes. The 2-(1-naphthalene)-pyridine−bicycloiridium complex is a red phosphor,[11] while its linkage isomer 2-(2-naphthalene)pyridine−bicycloiridium complex is a yellow phosphor. In this paper, we introduced the two linkage isomers into the polyfluorene backbone. The complex monomers (1-npyBr)$_2$Ir(tmd) and (2-npyBr)$_2$Ir(tmd) are with 2,2,6,6-tetramethyl-3,5-heptanedione as the bidentate ancillary ligand for better solubility in copolymerization.

[†] South China University of Technology.
[‡] Inspection Center on Chemicals, Minerals & Metallic Materials.
* Corresponding author: e-mail pswyang@scut.edu.cn.

10.1021/ma052057h CCC: $33.50
Published on Web 02/09/2006

Experimental Section

Measurements. ^{1}H and ^{13}C NMR spectra were recorded on a Bruker DRX 400 spectrometer operating respectively at 400 and 100 MHz, in deuterated chloroform solution with tetramethylsilane as a reference. The molecular weight of the polymers was determined by a Waters GPC 2410 in tetrahydrofuran (THF). Number-average (M_n) and weight-average (M_w) molecular weights were estimated by using a calibration curve of polystyrene standards. Elemental analyses were performed on a Vario EL elemental analysis instrument (Elementar Co.). The iridium content analyses were determined by using a Philips (Magix PRO) sequential X-ray fluorescence spectrometry (XRF), with a rhodium tube operated at 60 kV and 50 mA, a LiF 200 crystal, and a scintillation counter. Tris(acetylacetonate)iridium (III) (Ir content is 38%, from Alfa Aesar Co.) was used as a internal reference specimen. Samples and specimen were pressed into homogeneous tablets ($\phi = 30$ mm) of compressed (375 MPa) powder of the copolymers. The basic requirement of quantitative X-ray fluorescence analysis is first to prepare suitable specimens from the samples to be analyzed and then to measure the intensity of the peak (I_p) of the element (Ir), since this intensity is related to the concentration by means of the calibration procedure. XRF is especially suited the quantitative and qualitative analysis of iridium, owing to its being nondestructive method; therefore, the measurement error can be avoided by sample treatment comparing with the inductively coupled plasma (ICP) method. The uncertainty in measurement result for iridium content by XRF is about ±0.02%. Mass spectra (MS) of 5-bromo-2-(1-naphthalene)pyridine and 5-bromo-2-(2-naphthalene)pyridine were obtained by CE Instruments Trace 2000 Series GC/MS, and the MS of the Ir complexes were taken with a Thermo Finigan LCQ DECA XP Series system. UV−vis absorption spectra were recorded on a HP 8453 spectrophotometer.

The PL quantum yields were measured from solid films of materials used here. They were performed using an Integrating Sphere IS080 (LabSphere) to collect the emitted light in all directions under the excitation of 325 nm line of a HeCd laser (Melles Griot). The thicknesses of the solid films, typically, were 100−200 nm. The standard measurement process is referred to previous publication.[12] PL spectra of the copolymers in thin film on quartz substrate were recorded on an Instaspec IV CCD spectrophotometer (Oriel Co.) under 325 nm excitation of a HeCd laser. Emission lifetime studies of the copolymers were measured with an Edinburgh FL-920 spectrometer. Polymer films (100 nm thick layer) were spin-coated from a toluene solution of polymer at 1300 rpm on glass substrates. The excitation source was a nanosecond flash lamp operating under an atmosphere of H_2 gas (0.40−0.50 bar, 1.2 ns fwhm, 40 kHz repetition rate), whose output was filtered through a monochromator prior to sample excitation. Microstructure of polymer film was investigated using a transmission electron microscope (TEM, Philips, CM300, at an accelerating voltage of 300 kV). Specimens for TEM observation were prepared from a dilute polymer solution coated on copper mesh. Surface morphology was investigated using tapping-mode atomic force microscopy (AFM) (Thermo. Auto Probe C P Res.). AFM measurements were performed in air at room temperature. Specimens (100 nm thick layer) were spun from a toluene solution of polymer (or blend) at 1300 rpm on indium tin oxide (ITO)-coated glass substrates.

Materials. All manipulations involving air-sensitive reagents were performed in the atmosphere of dry argon. The solvents (THF, toluene) were purified by routine procedure and distilled under dry argon before being used. All reagents, unless otherwise specified, were obtained from Aldrich, Acros, and TCI Chemical Co. and used as received.

5-Bromo-2-(1-naphthalene)pyridine was synthesized by the procedure as follows: 2,5-Dibromopyridine (2.37 g, 10 mmol), 1-naphthaleneboronic acid (1.72 g, 10 mmol), and tetrakis-(triphenylphosphine)palladium (0.107 g, 0.1 mmol) were dissolved in toluene (15 mL) and ethanol (5 mL). Then an aqueous solution of 2 M Na_2CO_3 (6 mL) was added to the mixture. The result mixture was allowed to stir at 100 °C for 24 h. The reaction mixture was concentrated by evaporation of solvents, and the residue was dissolved in dichloromethane, washed with water, and dried under anhydrous sodium carbonate. After the evaporation of solvent, the obtained product was purified by column chromatography (silica gel, dichloromethane/hexane = 1:4) (yield: 70%). $m/z = 284$. ^{1}H NMR (400 MHz, $CDCl_3$) δ (ppm): 8.86 (s,1H), 8.04 (d, $^3J = 8.6$, 1H), 8.00 (d, $^3J = 2.9$, 1H), 7.96 (d, $^3J = 3.2$, 1H), 7.92 (d, $^3J = 3.2$, 1H), 7.62 (d, $^3J = 2.6$, 1H), 7.60 (d, $^3J = 2.8$, 1H), 7.50 (t, $^3J = 6.0$, 1H), 7.49 (t, $^3J = 6.0$, 1H), 7.47 (t, $^3J = 6.0$, 1H). Element Anal. Calcd for $C_{15}H_{10}BrN$ (%): C, 63.38; H, 3.52; N, 4.93. Found (%): C, 63.30; H, 3.45; N, 4.98.

5-Bromo-2-(2-naphthalene)pyridine was prepared following the similar procedure as above. $m/z = 284$. ^{1}H NMR (400 MHz; $CDCl_3$) δ (ppm): 8.79 (s,1H), 8.45 (s,1H), 8.10 (d, $^3J = 6.9$, 1H), 7.93 (d, $^3J = 8.2$, 1H), 7.92 (d, $^3J = 8.2$, 1H), 7.88 (d, $^3J = 3.3$, 1H), 7.86 (d, $^3J = 3.3$, 1H), 7.75 (d, $^3J = 8.5$, 1H), 7.52 (t, $^3J = 3.7$, 2H). Element Anal. Calcd for $C_{15}H_{10}BrN$ (%): C, 63.38; H, 3.52; N, 4.93. Found (%): C, 63.34; H, 3.43; N, 4.99.

Iridium(III) Bis(5-bromo-2-(1-naphthalene)pyridine-*C*$^{2'}$,*N*)-2,2,6,6-tetramethyl-3,5-heptanedione [(1-npyBr)$_2$Ir(tmd)] (1) was prepared according to the published procedures.[13] Iridium trichloride hydrate (178 mg, 0.56 mmol), 5-bromo-2-(1-naphthalene)pyridine (477 mg,1.68 mmol), 2-ethoxyethanol (15 mL), and water (5 mL) were added into a three-neck flask (100 mL). The mixture was refluxed under an argon atmosphere for 24 h and then cooled to room temperature. A red precipitate was filtered and washed with water and ethanol several times. The resulted red solid was purified by recrystallization in mixture of CH_2Cl_2 and hexane. Then the dried product (476 mg, 0.078 mmol) was mixed with 2,2,6,6-tetramethyl-3,5-heptanedione (40.5 mg, 0.22 mmol) and sodium carbonate (13 mg) in degassed 2-ethoxyethanol (8 mL) in a three-neck flask. The mixture was refluxed in an argon atmosphere for 13 h. After cooling to room temperature the red precipitate was formed. After being filtered and washed with water and methanol, the precipitate was purified by column chromatography (silica gel, dichloromethane) to get the red needle crystal product (yield: 75%). M−M(tmd), $IrL_2^+ = 759.2$. ^{1}H NMR (400 MHz; $CDCl_3$) δ (ppm): 8.53 (s, 2H), 8.44 (d, $^3J = 8.6$, 2H), 8.37 (d, $^3J = 9.0$, 2H), 7.88 (d, $^3J = 7.0$, 2H), 7.65 (d, $^3J = 8.0$, 2H), 7.46 (t, $^3J = 7.0$, 2H), 7.28 (t, $^3J = 7.8$, 2H), 7.07 (d, $^3J = 8.3$, 2H), 6.52 (d, $^3J = 8.3$, 2H), 5.56 (s, 1H), 0.91 (s, 18H). Element Anal. Calcd for $C_{41}H_{37}Br_2IrN_2O_2$ (%): C, 52.30; H, 3.93; N, 2.98. Found (%): C, 52.12; H, 3.79; N, 3.07.

Iridium(III) Bis(2-(1-naphthalene)pyridine-*C*$^{2'}$,*N*)-2,2,6,6-tetramethyl-3,5-heptanedione [(1-npy)$_2$Ir(tmd)] (2) M−M(tmd), $IrL_2^+ = 601.3$. ^{1}H NMR (400 MHz; $CDCl_3$) δ (ppm): 8.53 (d,$^3J = 8.7$, 2H), 8.48 (d, $^3J = 8.3$, 2H), 8.46 (d, $^3J = 6.7$, 2H), 7.78 (t, $^3J = 5.8$, 2H), 7.63 (d, $^3J = 7.9$, 2H), 7.45 (t, $^3J = 8.3$, 2H), 7.24 (t, $^3J = 7.0$, 2H), 7.08 (d, $^3J = 7.1$, 2H), 7.04 (t, $^3J = 8.3$, 2H),6.53 (t, $^3J = 8.3$, 2H), 5.50 (s, 1H), 0.87 (s, 18H). Element Anal. Calcd for $C_{41}H_{39}IrN_2O_2$ (%): C, 62.83; H, 4.98; N, 3.58. Found (%): C, 62.47; H, 4.82; N, 3.61.

Iridium(III) Bis(5-bromo-2(2-naphthalene)pyridine-*C*$^{2'}$,*N*)-2,2,6,6-tetramethyl-3,5-heptanedione [(2-npyBr)$_2$Ir(tmd)] (3) M−M(tmd), $IrL_2^+ = 759.2$. ^{1}H NMR (400 MHz; $CDCl_3$) δ (ppm): 8.60 (s,2H), 8.04 (s,2H), 7.96 (d, $^3J = 9.2$, 2H), 7.94 (d, $^3J = 9.2$, 2H), 7.65 (d, $^3J = 8.0$, 2H), 7.30 (d, $^3J = 7.9$, 2H), 7.16 (t, $^3J = 8.1$, 2H), 7.12 (t, $^3J = 8.0$, 2H), 6.67 (s, 2H), 5.57 (s, 1H), 0.93 (s, 18H). Element Anal. Calcd for $C_{41}H_{37}Br_2IrN_2O_2$ (%): C, 52.30; H, 3.93; N, 2.98. Found (%): C, 52.15; H, 3.76; N, 3.11.

Iridium(III) Bis(2-(1-naphthalene)pyridine-*C*$^{2'}$,*N*)-2,2,6,6-tetramethyl-3,5-heptanedione [(2-npy)$_2$Ir(tmd)] (4) M−M(tmd), $IrL_2^+ = 601.3$. ^{1}H NMR (400 MHz; $CDCl_3$) δ (ppm): 8.51 (d, $^3J = 6.0$ Hz, 2H), 8.10 (s, 2H), 8.09 (d, $^3J = 8.1$, 2H), 8.06 (s, 2H), 7.81 (t, $^3J = 8.5$, 2H), 7.66 (d, $^3J = 7.8$, 2H), 7.25 (d, $^3J = 7.7$, 2H), 7.16 (t, $^3J = 6.1$, 2H), 7.12 (t, $^3J = 6.2$, 2H), 6.69 (t, 2H), 5.50 (s, 1H), 0.89 (s, 18H). Element Anal. Calcd for $C_{41}H_{39}IrN_2O_2$ (%): C, 62.83; H, 4.98; N, 3.58. Found (%): C, 62.67; H, 4.76; N, 3.74.

General Procedures of Suzuki Polycondensation Taking PF1−NpyIrm1 (7) as an Example.[14] 2,7-Bis(4,4,5,5-tetramethyl-1,3,2-dioxaborolan-2-yl)-9,9-dioctylfluorene (**5**)[15] (341 mg, 0.5 mmol), 2,7-dibromo-9,9-dioctylfluorene (**6**)[16] (268 mg, 0.49 mmol), $(1\text{-npyBr})_2$Ir(tmd) (9.41 mg, 0.01 mmol), and bis(tri-*o*-tolyphosphine)palladium(II) dichloride (5 mg) were dissolved in the mixture of toluene/THF (15 mL), stirred for 0.5 h, and then Et_4NOH (20%) aqueous solution (4 mL) was added. The mixture was heated to 100 °C and stirred for 2 days in an argon atmosphere. Then the polymer was capped by adding 2-(4,4,5,5-tetramethyl-1,3,2-dioxaborolan-2-yl)-9,9-dioctylfluorene (50 mg) by continuous stirring for 12 h and then bromobenzene (0.25 mL) followed by continuous reacting for another 12 h. The whole mixture was poured into methanol. The precipitated polymer was recovered by filtration and purified by silica column chromatography with toluene to remove small molecular complex and catalyst residue (yield: 50%). Element Anal. Calcd (%): C, 89.16; H, 10.20; N, 0.071. Found (%): C, 88.53; H, 10.69; N, <0.3.

PF1−NpyIrm05 (8): Monomer feed ratio: 2,7-bis(4,4,5,5-tetramethyl-1,3,2-dioxaborolan-2-yl)-9,9-dioctylfluorene (0.5 mol), 2,7-dibromo-9,9-dioctylfluorene (0.495 mol), and $(1\text{-npyBr})_2$Ir(tmd) (0.005 mol) (yield: 56%). Element Anal. Calcd (%): C, 89.42; H, 10.25; N, 0.036. Found (%): C, 89.25; H, 10.41; N, <0.3.

PF1−NpyIrm2 (9): Monomer feed ratio: 2,7-bis(4,4,5,5-tetramethyl-1,3,2-dioxaborolan-2-yl)-9,9-dioctylfluorene (0.5 mol), 2,7-dibromo-9,9-dioctylfluorene (0.48 mol), and $(1\text{-npyBr})_2$Ir(tmd) (0.02 mol) (yield: 50%). Element Anal. Calcd (%): C, 88.64; H, 10.09; N, 0.14. Found (%): C, 88.11; H, 10.39; N, <0.3.

PF1−NpyIrm5 (10): Monomer feed ratio: 2,7-bis(4,4,5,5-tetramethyl-1,3,2-dioxaborolan-2-yl)-9,9-dioctylfluorene (0.5 mol), 2,7-dibromo-9,9-dioctylfluorene (0.45 mol), and $(1\text{-npyBr})_2$Ir(tmd) (0.05 mol) (yield: 49%). ^{1}H NMR (400 MHz, $CDCl_3$) δ (ppm): 8.64 (pyridine ring); 8.13, 7.84, 7.69 (fluorene ring); 7.52,7.38, 7.11, 6.88 (naphthylpyridine ring); 5.83 (H-diketone); 2.12, 1.51−1.34, 1.16,0.91−0.75 (H-alkyl). ^{13}C NMR (100 MHz, $CDCl_3$) δ (ppm): 151.81, 140.49, 140.03, 128.78, 126.95, 126.66, 126.16, 122.82, 121.50, 120.00, 119.60, 77.33, 77.21, 77.01, 76.69, 55.35, 40.39, 31.94, 31.80, 30.04, 29.71, 29.23, 28.38, 27.42, 23.93, 23.72, 22.61, 14.07. Element Anal. Calcd (%): C, 87.13; H, 9.79; N, 0.343. Found (%): C, 87.15; H, 10.09; N, <0.3.

PF2−NpyIrm1 (11): Monomer feed ratio: 2,7-bis(4,4,5,5-tetramethyl-1,3,2-dioxaborolan-2-yl)-9,9-dioctylfluorene (0.5 mol), 2,7-dibromo-9,9-dioctylfluorene (0.49 mol), and $(2\text{-npyBr})_2$Ir(tmd) (0.01 mol) (yield: 55%). Element Anal. Calcd (%): C, 89.16; H, 10.20; N, 0.071. Found (%): C, 88.47; H, 10.71; N, <0.3.

PF2−NpyIrm2 (12): Monomer feed ratio: 2,7-bis(4,4,5,5-tetramethyl-1,3,2-dioxaborolan-2-yl)-9,9-dioctylfluorene (0.5 mol), 2,7-dibromo-9,9-dioctylfluorene (0.48 mol), and $(2\text{-npyBr})_2$Ir(tmd) (0.02 mol) (yield: 53%). Element Anal. Calcd (%): C, 88.64; H, 10.09; N, 0.14. Found (%): C, 88.24; H, 10.29; N, <0.3.

PF2−NpyIrm5 (13): Monomer feed ratio: 2,7-bis(4,4,5,5-tetramethyl-1,3,2-dioxaborolan-2-yl)-9,9-dioctylfluorene (0.5 mol), 2,7-dibromo-9,9-dioctylfluorene (0.45 mol), and $(2\text{-npyBr})_2$Ir(tmd) (0.05 mol) (yield: 51 %). ^{1}H NMR (100 MHz,$CDCl_3$) δ (ppm): 8.68 (pyridine ring); 8.21, 8.17, 7.85 (fluorene ring); 7.82, 7.77, 7.52, 7.26, 6.95 (2-naphthylpyridine ring); 5.75 (H-diketone); 2.14,1.54, 1.27−1.15, 0.99, 0.85 (H-alkyl). ^{13}C NMR (100 MHz, $CDCl_3$) δ (ppm): 151.82, 140.51, 140.33, 140.03, 128.79, 127.21, 126.17, 126.04, 121.50, 119.97, 77.33, 77.22, 77.01, 76.70, 55.35, 40.39, 31.80, 30.05, 29.71, 29.24, 28.43, 27.42, 23.93, 22.71, 22.61, 14.08. Element Anal. Calcd (%): C, 87.13; H, 9.79; N, 0.343. Found (%): C, 87.32; H, 10.16; N, <0.3.

PF2−NpyIrm7 (14): Monomer feed ratio: 2,7-bis(4,4,5,5-tetramethyl-1,3,2-dioxaborolan-2-yl)-9,9-dioctylfluorene (0.5 mol), 2,7-dibromo-9,9-dioctylfluorene (0.43 mol), and $(2\text{-npyBr})_2$Ir(tmd) (0.07 mol) (yield: 50%). Element Anal. Calcd (%): C, 86.18; H, 9.58; N, 0.470. Found (%): C, 86.42; H, 9.81; N, 0.30.

LED Fabrication and Characterization. Polymers were dissolved in *p*-xylene and filtered with a 0.45 μm filter. Patterned ITO-coated glass substrates were cleaned with acetone, detergent, distilled water, and 2-propanol, subsequently in an ultrasonic bath. After treatment with oxygen plasma, 150 nm of poly(3,4-ethylenedioxythiophene) (PEDOT) doped with poly(styrenesulfonic acid) (PSS) (Batron-P 4083, Bayer AG) was spin-coated onto the ITO substrate followed by drying in a vacuum oven at 80 °C for 8 h. A thin film of polymers was coated onto the anode by spin-casting inside a drybox. The film thickness of the active layers was around 75−80 nm, measured with an Alfa Step 500 surface profiler (Tencor). A thin layer of Ba (4−5 nm) and subsequently 200 nm layer of Al were vacuum-evaporated subsequently on the top of an EL polymer layer in a vacuum of 1×10^{-4} Pa. Device performances were measured inside a drybox. Current−voltage ($I-V$) characteristics were recorded with a Keithley 236 source meter. EL spectra were obtained by Oriel Instaspec IV CCD spectrograph. Luminance was measured by a PR 705 photometer (Photo Research). The external quantum efficiencies were determined by a Si photodiode with calibration in an integrating sphere (IS080, Labsphere).

Results and Discussion

Synthesis and Chemical Characterization. The synthetic routes of the complex monomers and the corresponding chelating copolymers are depicted in Scheme 1. Two linkage isomers of naphthylpyridine were synthesized with Suzuki coupling reaction by 2,5-dibromopyridine or 2-bromopyridine and isomers of naphthaleneboronic acid with high yield. The corresponding iridium complexes were synthesized by chloride-bridged iridium dimers with 2,2,6,6-tetramethyl-3,5-heptanedione (Htmd) in the presence of sodium carbonate. Because of the better solubility of the bicycloiridium complex $(1\text{-npyBr})_2$Ir(tmd) and $(2\text{-npyBr})_2$Ir(tmd) in organic solvent, the target polymers can be obtained by Suzuki polycondensation of A−A- and B−B-type monomers. The corresponding complexes without bromine substitution in ligands, $(1\text{-npy})_2$Ir(tmd) and $(2\text{-npy})_2$Ir(tmd), were prepared for comparison, the complexes being respectively predigested as NpyIrm and 2-NpyIrm for convenience. The chelating copolymers of different-composition complexes were prepared from 2,7-dibromo-9,9-dioctylfluorene, 2,7-bis(4,4,5,5-tetramethyl-1,3,2-dioxaborolan-2-yl)-9,9-dioctylfluorene, and complexes by Suzuki polycondensation. The feed ratios of complexes in the polycondensation were 0.5, 1, 2, 5, and 7 mol %, and the corresponding copolymers were named PF1−NpyIrm05, PF1−NpyIrm1, PF1−NpyIrm2, PF1−NpyIrm5, and PF2−NpyIrm1, PF2−NpyIrm2, PF2−NpyIrm5, and PF2−NpyIrm7, respectively. The iridium contents in polymers were estimated by X-ray fluorescence spectrometry (XRF); therefore, the molar ratios of Ir complexes incorporated into copolymers were calculated by combining XRF data with the elemental analyses of carbon and hydrogen (Table 1). The results indicate that the actual Ir complex contents in the copolymers are slightly lower than the complex monomer feed ratios. The number-average molecule weights (M_n) of the most copolymers are higher than 30 000 with the narrow polydispersity index (PDI) from 1.22 to 1.43 (Table 1).

Photophysical Properties. Two linkage isomers of naphthylpyridine in which the pyridine groups are linked to the C_1 or C_2 carbons of naphthalene, 2-(1-naphthalene)pyridine, and 2-(2-naphthalene)pyridine are used to prepare Ir complexes. The complexes with the different sizes of the ligand π- system show various optical (Figure 1) and electroluminescent properties.[17] Figure 1 shows UV−vis absorption and PL spectra of the complexes. All of the phosphors show a remarkably strong absorption band in the region of 440−520 nm, which can be assigned to a spin-forbidden triplet metal-to-ligand charge-transfer (^{3}MLCT) band of the complexes.[18] In the PL spectra of NpyIrm and 2-NpyIrm, NpyIrm exhibits a single emission with the peak maximum at 610 nm, whereas its linkage isomer

Scheme 1. Synthetic Routes of the Complex Monomers and Chelating Copolymers

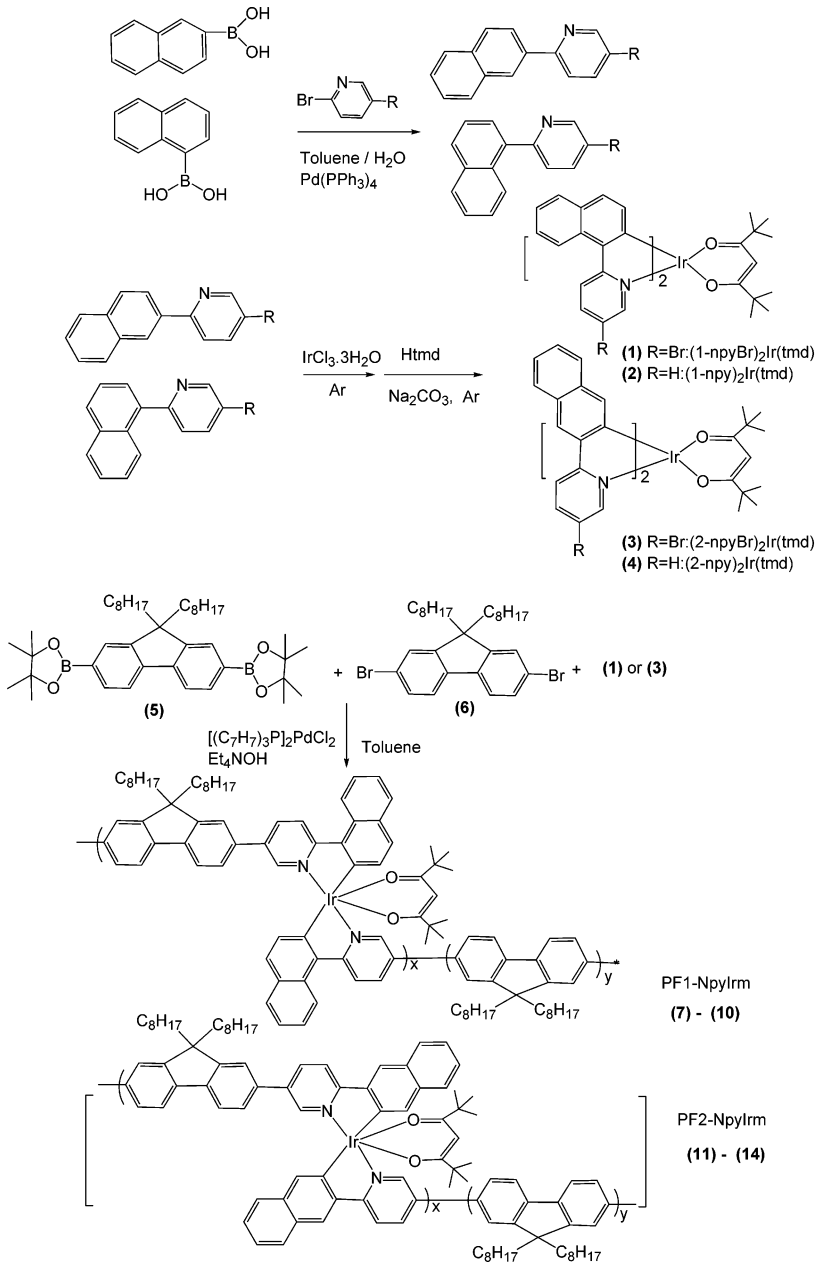

Table 1. Molecular Weights and Composition of the Copolymers

polymer	M_n ($\times 10^3$)	PDI	complex content (mol %) in feed ratio	complex content (mol %) in polymer[a]
PFO	23.1	2.47		
PF1−NpyIrm05	33.1	1.34	0.5	0.41
PF1−NpyIrm1	35.8	1.30	1	0.98
PF1−NpyIrm2	32.7	1.22	2	1.59
PF1−NpyIrm5	32.6	1.36	5	4.23
PF2−NpyIrm1	31.2	1.42	1	0.83
PF2−NpyIrm2	30.7	1.39	2	1.48
PF2−NpyIrm5	21.7	1.43	5	3.20
PF2−NpyIrm7	22.0	1.42	7	4.12

[a] Calculated from the carbon, hydrogen, and iridium content in copolymers.

2-NpyIrm shows an emission with the peak maximum at 570 nm.

For the chelating electrophosphorescent polymers, the overlapping between PL emission of the host polymer and the absorption spectra of pristine complexes is not suitable to show the energy matching condition because the ligands of complex units changed into the other moieties when covalently linked onto conjugated polymer backbone. It is reasonable to use the absorption of the complexes units in copolymers as the "real complexes". UV−vis absorption of the chelating copolymers (PF1−NpyIrm5 and PF2−NpyIrm7) and the PL spectrum of

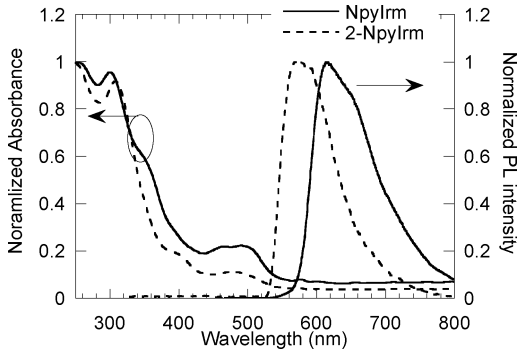

Figure 1. UV−vis absorption of the complexes in film and PL spectra of the complexes in CH_2Cl_2 solution (10^{-1} mol/L).

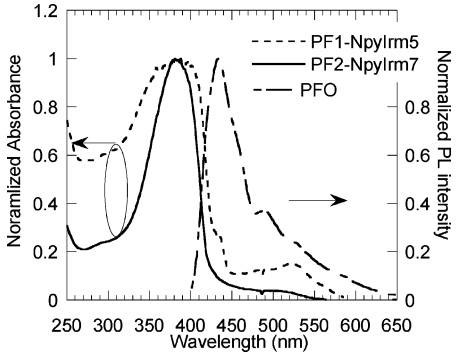

Figure 2. UV−vis absorption of the copolymers and PL spectra of host polymer in film.

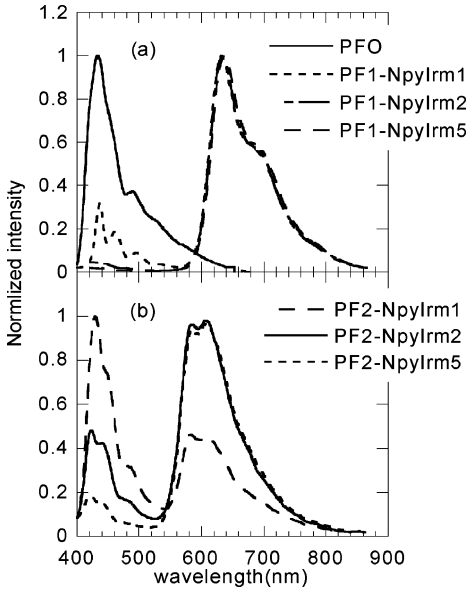

Figure 3. PL spectra of the chelating copolymers in film: (a) PF1−NpyIrm; (b) PF2−NpyIrm.

Table 2. Photoluminescent Properties of the Copolymers and Complexes in Film

		photoluminescence	
polymer	$\lambda_{abs\ max}$ (nm)	λ_{PL} (nm)	Q_{PL} (%)
NpyIrm	300, 350, 500	610	1.0
2-NpyIrm	310, 400, 480	570	0.3
PFO	380	430	42
PF1−NpyIrm1	380	430, 630	18.8
PF1−NpyIrm2	380	430, 630	22.2
PF1−NpyIrm5	380, 520	630	18.5
PF2−NpyIrm1	380	430, 590	4.9
PF2−NpyIrm2	380	430, 590	4.6
PF2−NpyIrm5	380	430, 590	3.7

the host polymer (PFO) are shown in Figure 2. The peak at around 380 nm, which comes from the fluorene segment, dominates UV−vis absorption of the chelating copolymers. The absorption peaks in the region of 450−550 nm can be assigned to a spin-forbidden triplet metal-to-ligand charge-transfer (^{3}MLCT) band of the complex unit in the copolymers. It seems that there is fitting overlapping between PL emission of the host polymer and the absorption spectra of the complex unit in copolymers.

PL spectra of the chelating copolymers PF1−NpyIrm are shown in Figure 3a. The maximum emission of the copolymers is about 630 nm, which are red-shifted around 20 nm compared with PL emission of the pristine complex NpyIrm (see Figure 1). The significant red shift in PL emission in the chelating

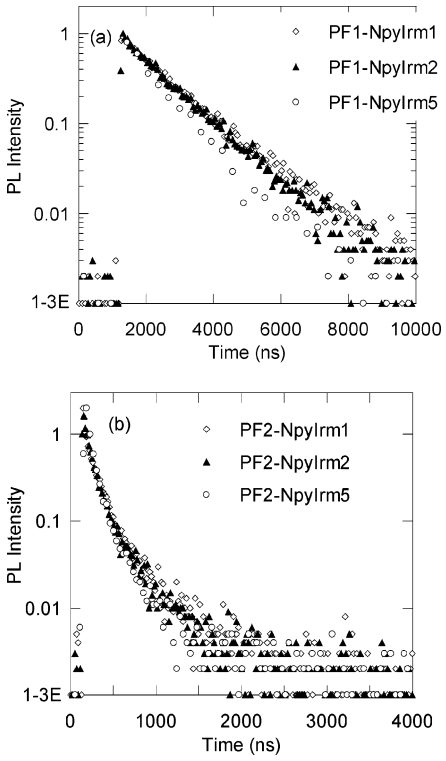

Figure 4. Transient PL response to a flash excitation (λ_{exc} = 390 nm): (a) at 630 nm from films of PF1−NpyIrm; (b) at 585 nm from films of PF2−NpyIrm.

copolymers synthesized in this study provides the evidence that Ir complexes are indeed incorporated into polymer main chain. The facts that the extended conjugated length in the ligand of phosphorescent complexes will generally shift PL emission to lower energy side were reported previously.[18b,19] PL spectra of chelating copolymers PF2−NpyIrm are shown in Figure 3b. The PL emission of the copolymers also red shifts around 20 nm compared with the emission of pristine complex 2-NpyIrm. In Figure 3a, the intense emission peaked at about 430 nm from host unit can be observed for those copolymers with low Ir complex content less than 5 mol %. This indicates that the energy transfer from fluorene segments to the Ir complex connected on the main chain is incomplete. The relative intensities at the peak of 430 nm vary with the Ir complex contents in the copolymers. With the increase of Ir complex content in copolymers, the emission intensity of 430 nm descends. The emission of fluorene segments in copolymers almost quenched completely for the copolymers with the Ir complex feed ratio of 5 mol %, which indicates that energy transfer from the host to the Ir complex becomes complete. Compared with copolymers PF1−NpyIrm, the energy transfer in copolymers PF2−NpyIrm is less effective (Figure 3b). In the covalently linked copolymers, under photoexcitation, the singlet excited states are created on the main chain and subsequently transfer to the metal−organic complex by intra- and intermolecular energy transfer. From Figure 2, we can see that the absorption spectrum of PF2−NpyIrm7 is more blue-shifted than that of PF1−NpyIrm5. The observed blue-shift suggests that 2-(2-naphthalene) moieties effectively decrease the conjugation length of polymer backbone, since the coplanarity of linear π-system is interrupted.[20] Therefore, we may speculate that better intramolecular energy transfer for PF1−NpyIrm might be due to longer conjugation length. In addition, the less overlapping between PL emission of host polymer and UV−vis absorption of the complex units in PF2−NpyIrm make

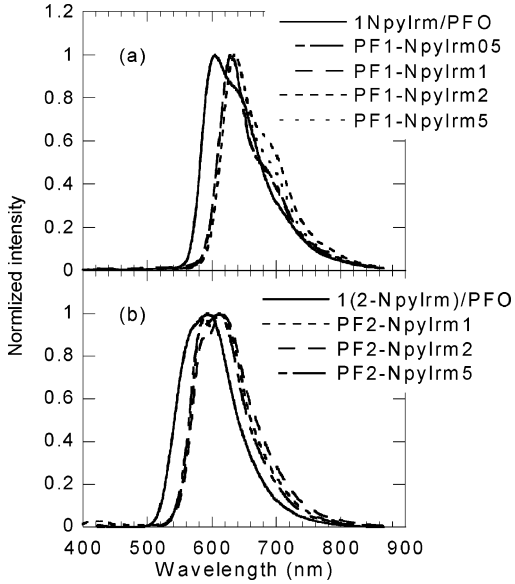

Figure 5. EL spectra of the chelating copolymers (a) PF1−NpyIrm and (b) PF2−NpyIrm. Device structure: ITO/PEDOT/PVK/polymer/Ba/Al.

Table 3. PL Lifetime of Copolymers in Film

polymer	lifetime τ_1 (μs)	lifetime τ_2 (μs)	χ^2	pump (monitor) (nm)
PF1−NpyIr1	1.342		1.117	390 (630)
PF1−NpyIr2	1.247		1.204	390 (630)
PF1−NpyIr5	1.021		1.224	390 (630)
PF2−NpyIr1	0.43	0.125	1.050	390 (585)
PF2−NpyIr2	0.37	0.089	1.009	390 (585)
PF2−NpyIr5	0.22	0.052	1.186	390 (585)

Förster energy transfer in polymer less effective. The PL efficiencies and the maximum emissions of the copolymers are shown in Table 2. The PL efficiencies of copolymers decrease with the increase of complex contents. The PL efficiencies of PF2−NpyIrm copolymers are much lower than that of the PF1−NpyIrm. Photoluminescent properties of the complexes in film are also shown in Table 2 because the complexes with branching substitution in the ligand can be spin-coated from the toluene solution. We can see that PL efficiencies of both complexes are much low, owing to the concentration quenching and T−T annihilation of pure complexes film. Photoluminescence decay studies were carried out to estimate the lifetime of the excited states. The PL decays of the polymers films are shown in Figure 4. The decay characteristics of the two series of polymers are distinct. The decay characteristics of the polymers PF1−NpyIrm are monoexponential with emission lifetime of about 1 μs, whereas the decay characteristics of the polymers PF2−NpyIrm are two-exponential with two lower lifetimes (Table 3).

Electrophosphorescent Properties. The double-layer devices were fabricated in the configuration ITO/PEDT/PVK/polymer/Ba/Al. Figure 5a shows EL spectra of the devices from chelating copolymers PF1−NpyIrm. The EL spectrum of the device from NpyIrm(1 mol %)-doped into PFO (1NpyIrm/PFO) is also shown as a comparison. The maximum EL emission of the doping system (1NpyIrm/PFO) is at 600 nm, whereas the EL emissions of the copolymers are about 630 nm. CIE (Commission Internationale de I'Eclairage) coordinates (0.65, 0.31) for the PF1−NpyIrm copolymers are within the scope of saturated red light (Table 3). EL spectra of PF2−NpyIrm copolymers are shown in Figure 5b. The maximum emissions of copolymers PF2−NpyIrm are in the region of 585−610 nm, which are almost same as their PL emissions. Compared with PL spectra (Figure 2), the emission of host segments at 430 nm in EL spectra is completely quenched for the copolymer with Ir complex content as low as 0.5 mol %. The fact that the complete quenching of host EL emission at lower Ir complex concentration than that of PL emission was presented by many authors,[21] which confirms that the dominant emission mechanism in such systems is charge trapping (rather than Förster energy transfer) followed by recombination on the Ir complex unit. Preliminary device performances are encouraging (Table 4). The best device performances are achieved from PF1−NpyIrm1. At a current density (J) of 5.2 mA/cm^2, the maximal external quantum efficiency (η_{ext}) of 7.0% is obtained with the luminance of 138 cd/m^2, and at a current density of 38 mA/cm^2, the value of η_{ext} reaches 6.5% with the luminance of 926 cd/m^2. To the best of our knowledge, this is the highest reported for the saturated red-light phosphorescent polymer emitters. Compared with copolymer PF1−NpyIrm1, the doping system 1NpyIrm/PFO with the same device structure has lower device performances. In Figure 6, the current density (J)−voltage (V) and the luminance (L)−bias voltage (V) for the devices from both the copolymer PF1−NpyIrm1 and the blend 1NpyIrm/PFO with the same Ir complex concentration (1 mol %) are compared. It is obvious that the device from chelating copolymer shows the

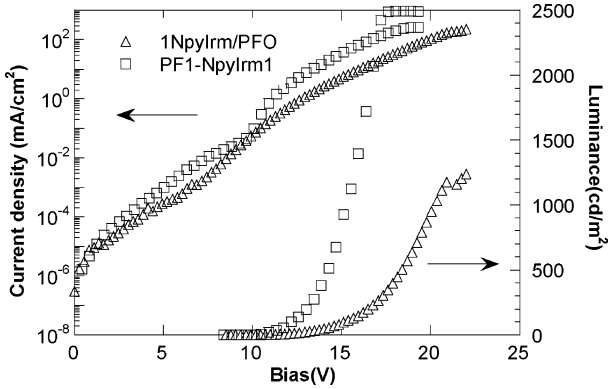

Figure 6. Comparison of $J-V$ and $L-V$ curves of the devices from copolymer, PF1−NpyIrm1, and blend, 1NpyIrm/PFO. Device structures: ITO/PEDOT/PVK/polymer (or blend)/Ba/Al.

Table 4. Device Performances of the Chelating Copolymers[a]

	J = 30 mA/cm^2				J = 100 mA/cm^2				CIE coordinates	
polymer	bias (V)	L (cd/m^2)	LE (cd/A)	QE_{ext} (%)	bias (V)	L (cd/m^2)	LE (cd/A)	QE_{ext} (%)	x	y
1NpyIrm/PFO	17.8	396	1.3	2.1	20.0	900	0.9	1.4	0.62	0.37
PF1−NpyIrm05	14.7	451	1.5	3.9	16.2	1242	1.3	3.3	0.65	0.31
PF1−NpyIrm1	15.1	732	2.5	6.5	16.5	2010	2.0	5.3	0.65	0.31
PF1−NpyIrm2	18.0	570	1.9	4.9	20.0	1560	1.6	4.1	0.66	0.30
PF1−NpyIrm5	15.6	602	2.0	5.2	18.0	1507	1.5	4.0	0.67	0.31
PF2−NpyIrm1	17.3	334	1.1	1.5	19.4	800	0.8	1.0	0.56	0.40
PF2−NpyIrm2	17.8	396	1.3	1.6	20.0	600	0.6	1.0	0.59	0.40
PF2−NpyIrm5	18.4	430	1.4	2.5	15.6	1136	1.1	1.9	0.56	0.43

[a] Device structure: ITO/PEDOT/PVK/polymer/Ba/Al.

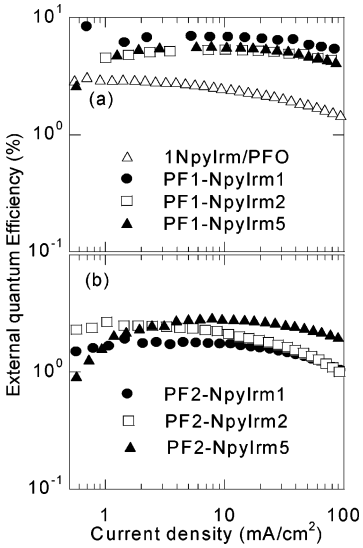

Figure 7. External quantum efficiencies vs current density: (a) PF1−NpyIrm; (b) PF2−NpyIrm. Device structure: ITO/PEDOT/PVK/polymer/Ba/Al.

sharper exponential rise in $J-V$ after turn-on, the lower operating voltage, and the higher efficiency. Other chelating copolymers show a similar tendency. This clearly indicates much better device performances from chelating polymers than blend systems.

Figure 7 shows the external quantum efficiency as a function of current density for the devices from these chelating copolymers. In Figure 7a, compared with the doping system (1NpyIrm/PFO), the copolymers have better stability at the high current density. At $J = 100$ mA/cm^2, the value of η_{ext} remains 5.3%, corresponding to a loss of only 18% from its value of $\eta_{ext} = 6.5\%$ at $J = 38$ mA/cm^2. In comparison, the external quantum efficiency of 1NpyIrm/PFO is 2.1% at $J = 30$ mA/cm^2, and it drops more quickly with increasing current ($\eta_{ext} = 1.4\%$ at $J = 100$ mA/cm^2), corresponding to a loss of 33%. This indicates that the chelating copolymers with Ir complex unit introduced onto the conjugated polymer backbone may have an advantage in the depression of concentration quenching[22] and T−T annihilation,[23] which are the primary origin of quenching mechanism for the blend system at a high current density. Of the two series of chelating copolymers, the copolymers PF1−NpyIrm have much better device performances than copolymers PF2−NpyIrm, which means that the selecting proper complex[10b] and the match of the complex with the host segment are significant to obtain the highly efficient electrophosphorescent copolymers.

Film Morphology. Since film morphologyis also related to the devices performances, the direct evidences of film microstructure are obtained by TEM and AFM. Figure 8 shows TEM images of the films from copolymer and the relative blend, respectively. The interphase from copolymer film is obscure with aggregate domains on the length scales of ∼20 nm (Figure 8a). Since iridium atom has a larger electron scattering cross than the carbon atom, the dark spots are likely to be Ir complex aggregates. On the other hand, the blend film shows a smooth interphase with the aggregate domains of ∼50 nm (Figure 8b), suggesting that the polymer film is more homogeneous with the fine-scale phase separation or aggregates. More direct surface

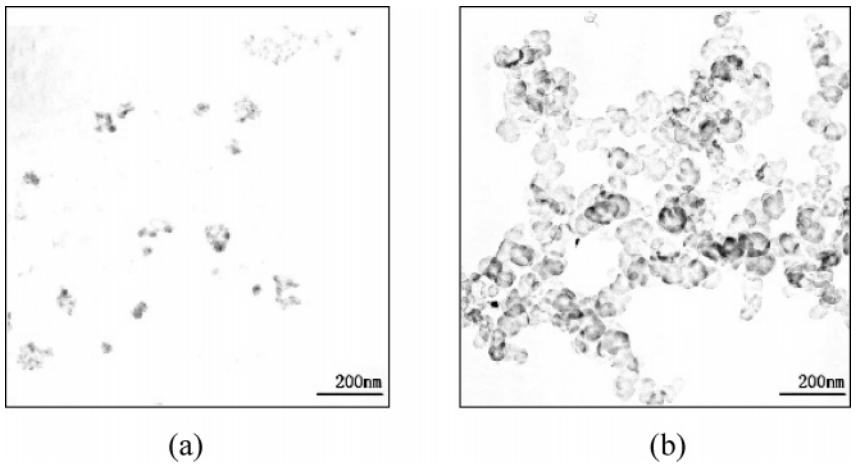

Figure 8. Typical TEM images of films of (a) polymer PF1−NpyIrm1 and (b) doping system 1NpyIrm/PFO.

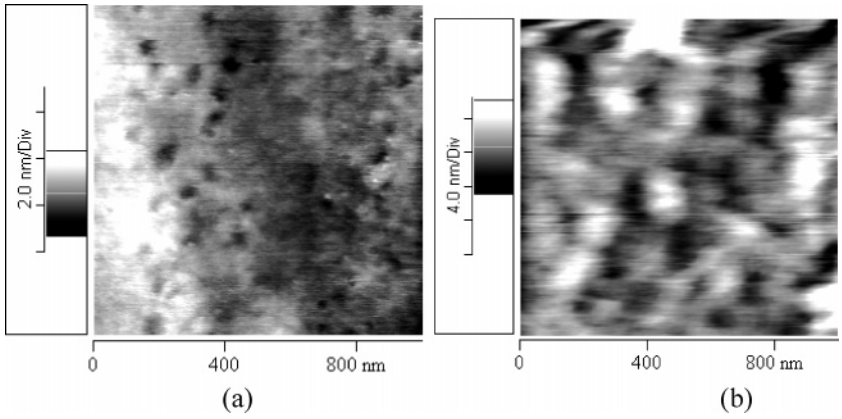

Figure 9. Tapping-mode AFM topographic images of films: (a) polymer PF1−NpyIrm1; (b) doping system 1NpyIrm/PFO.

topographies of the films are investigated by AFM and shown in Figure 9. The polymer film shows an aggregate domain with a horizontal size of ~50 nm and a vertical root-mean-square (rms) roughness in the range of 0.9 nm (Figure 9a), and the blend film shows a more obvious aggregation with a horizontal size of ~100 nm and a rms roughness in the range of 1.4 nm (Figure 9b). These results clearly indicate that phase separation existed in both the polymer and the doped system, owing to the immiscibility between the host and the guest materials.[24] The formation of aggregates in the phosphorescent dye doped device results in lower efficiency for the phosphorescent dye-doped devices.[25] Therefore, the homogeneous dispersion and fine-scale phase separation or aggregates of a dopant in a host polymer must be addressed to fabricate efficient devices.

Conclusion

In summary, a series of phosphorescent chelating copolymers based on the linkage isomers of naphthylpyridine−iridium complexes were synthesized by Suzuki polycondensation of A−A- and B−B-type monomers. Chemical and photophysical characterizations confirm that Ir complexes have been indeed incorporated into polymer backbone. Because of the extended conjugate length of the complexes in conjugation with a neighboring conjugate segment in the polymer backbone, the chelating copolymers take advantage of adjusting to the saturated red light emitting. The best device performances were achieved from PF1−NpyIrm1 at a current density of 38 mA/cm^2, and the external quantum efficiency reached 6.5% with a luminance of 926 cd/m^2 at the emission peak of 630 nm. No remarkable efficiency decay with the increase in current density shows that the chelating copolymers are promising candidate materials for PHPLEDs.

Acknowledgment. The authors are grateful to the Ministry of Science and Technology of China (No. 2002CB613403) and the National Natural Science Foundation of China (No. 50173008 and No. 20574021) for their financial support to our work.

References and Notes

(1) (a) Ma, Y. G.; Zhang, H. Y.; Shen, J. C.; Chen, C. M. *Synth. Met.* **1998**, *94*, 245. (b) Baldo, M. A.; O'Brien, D. F.; You, Y.; Shoustikov, A.; Sibley, S.; Thompson, M. E.; Forrest, S. R. *Nature (London)* **1998**, *395*, 151. (c) O'Brien, D. F.; Baldo, M. A.; Thompson, M. E.; Forrest, S. R. *Appl. Phys. Lett.* **1999**, *74*, 442. (d) Adachi, C.; Baldo, M. A.; Forrest, S. R.; Thompson, M. E. *Appl. Phys. Lett.* **2000**, *77*, 904. (e) Wang, Y.; Herron, N.; Grushin, V. V.; Lecloux, D.; Petrov, V. *Appl. Phys. Lett.* **2001**, *79*, 449. (f) Adachi, C.; Baldo, A. M.; Forrest, S. R.; Lamansky, S.; Thompson, M. E.; Kwong, R. C. *Appl. Phys. Lett.* **2001**, *78*, 1622. (g) Jiang, X. Z.; Jen, A. K.-Y.; Carlson, B.; Dalton, L. R. *Appl. Phys. Lett.* **2002**, *80*, 713. (h) Stathatos, E.; Lianos, P.; Evgeniou, E.; Keramidas, A. D. *Synth. Met.* **2003**, *139*, 2433.

(2) Namdas, E. B.; Ruseckas, A.; Samuel, I. D. W.; Lo, S.; Burn, P. L. *J. Phys. Chem. B* **2004**, *108*, 1570.

(3) Lee, C. L.; Kang, N. G.; Cho, Y. S.; Lee, J. S.; Kim, J. J. *Opt. Mater.* **2003**, 21119.

(4) Tokito, S.; Suzuki, M.; Sato, F.; Kamachi, M.; Shirane, K. *Organ. Electron.* **2003**, *4*, 105.

(5) Chen, X.; Liao, J.-L.; Liang, Y.; Ahmed, M. O.; Tseng, H.-E.; Chen, S.-A. *J. Am. Chem. Soc.* **2003**, *125*, 636.

(6) Jiang, J. X.; Jiang, C. Y.; Yang, W.; Zhen, H. Y.; Huang, F.; Cao, Y. *Macromolecules* **2005**, *38*, 4072.

(7) Sandee, A. J.; Williams, C. K.; Evans, N. R.; Davies, J. E.; Boothby, C. E.; Köhler, A.; Friend, R. H.; Holmes, A. B. *J. Am. Chem. Soc.* **2004**, *126*, 7041.

(8) Zhen, H. Y.; Jiang, C. Y.; Yang, W.; Jiang, J. X.; Huang, F.; Cao, Y. *Chem.—Eur. J.* **2005**, *11*, 5007.

(9) (a) Hou, Q.; Xu, Y.; Yang, W.; Yuan, M.; Peng, J.; Cao, Y. *J. Mater. Chem.* **2002**, *12*, 2887. (b) Yang, R.; Tian, R.; Hou, Q.; Yang, W.; Cao, Y. *Macromolecules* **2003**, *36*, 7453.

(10) (a) Tamayo, A. B.; Alleyne, B. D.; Djurovich, P. I.; Lamansky, S.; Tsyba, I.; Ho, N. N.; Bau, R.; Thompson, M. E. *J. Am. Chem. Soc.* **2003**, *125*, 7377. (b) Li, C.-L.; Su, Y.-J.; Tao, Y.-T.; Chou, P.-T.; Chien, C.-H.; Cheng, C.-C.; Liu, R.-S. *Adv. Funct. Mater.* **2005**, *15*, 387.

(11) Zhu, W. G.; Zhu, M. X.; Ke, Y.; Su, L. J.; Yuan, M.; Cao, Y. *Thin Solid Films* **2004**, *446*, 128.

(12) Greenham, N. C.; Samuel, I. D. W.; Hayes, G. R.; Philips, R. T.; Kessener, Y. A. R. R.; Moratti, S. C.; Holmes, A. B.; Friend, R. H. *Chem. Phys. Lett.* **1995**, *241*, 89.

(13) Lamansky, S.; Djurovich, P.; Murphy, D.; Abdel-Razzaq, F.; Kwong, R.; Tsyba, I.; Bortz, M.; Mui, B.; Bau, R.; Thompson, M. E. *Inorg. Chem.* **2001**, *40*, 1704.

(14) (a) Rees, I. D.; Robinson, K. L.; Holmes, A. B.; Towns, C. R.; O'Dell, R. *MRS Bull.* **2002**, *27*, 451. (b) Allen, I.; Pounds, T.; Murtagh, L.; Wallace, P.; Towns, C. WO 035796 A1, 2003.

(15) (a) Rondeau, M. D.; Leclerc, M. *Macromolecules* **1997**, *30*, 7686. (b) Yang, W.; Hou, Q.; Liu, C. Z.; Niu, Y. H.; Huang, J.; Yang, R. Q.; Cao, Y. *J. Mater. Chem.* **2003**, *13*, 1351.

(16) (a) Woo, E. P.; Inbasekaran, M.; Shiang, W.; Roof, G. R. WO 97/05184, 1997. (b) Lee, J. K.; Klaerner, G.; Miller, R. D. *Chem. Mater.* **1997**, *11*, 11083.

(17) Lamansky, S.; Djurovich, P.; Murphy, D.; Abdel-Razaq, F.; Lee, H.-E.; Adachi, C.; Burrows, P. E.; Forrest, S. R.; Thompson, M. E. *J. Am. Chem. Soc.* **2001**, *123*, 4304.

(18) (a) Colombo, M. G.; Hauser, A.; Gudel, H. U. *Inorg. Chem.* **1993**, *32*, 3088. (b) Schimid, B.; Garces, F. O.; Watts, R. J. *Inorg. Chem.* **1994**, *33*, 9.

(19) (a) Chen, F. C.; Yang, Y.; Thompson, M. E.; Kido, J. *Appl. Phys. Lett.* **2002**, *80*, 2308. (b) Gong, X.; Ostrowski, J. C.; Moses, D.; Bazan, G. C.; Heeger, A. J. *Adv. Funct. Mater.* **2003**, *13*, 439.

(20) Tammer, M.; Horsburgh, L.; Monkman, A. P.; Brown, W.; Burrows, H. D. *Adv. Func. Mater.* **2002**, *12*, 447.

(21) (a) Zhu, W. G.; Mo, Y. Q.; Su, L. J.; Yang, W.; Cao, Y. *Appl. Phy. Lett.* **2002**, *80*, 2045. (b) Lane, P. A.; Palilis, L. C.; O'Brien, D. F.; Giebeler, C.; Cadby, A. J.; Lidzey, D. G.; Campbell, A. J.; Blau, W.; Bradley, D. D. C. *Phys. Rev. B* **2001**, *63*, 235206. (c) Tessler, N.; Cleave, P. K. H. V.; Pinner, D. J.; Friend, R. H.; Yahioglu, G.; Barny, P. Le.; Gray, J.; Souza, M. D.; Rumbles, G. *Thin Solid Films* **2000**, 363.

(22) (a) Guo, J.; Ye, K.; Wu, Y.; Liu, Y.; Wang, Y. *Synth. Met.* **2003**, *137*, 1075. (b) Hong, Z. R.; Lee, C. S.; Lee, S. T.; Li, W. L.; Liu, S. Y. *Appl. Phys. Lett.* **2003**, *82*, 2218.

(23) (a) Baldo, M. A.; Adachi, C.; Forrest, S. R. *Phys. Rev. B* **2000**, *62*, 10967. (b) Adachi, C.; Kwong, R. C.; Djurovich, P.; Thompson, M. E.; Forrest, S. R. *Appl. Phys. Lett.* **2001**, *79*, 2082.

(24) Chen, F.-F.; Chang, S.-C.; He, G.; Pyo, S.; Yang, Y. *J. Polym. Sci., Part B* **2003**, *41*, 2681.

(25) Noh, Y.-Y.; Lee, C.-L.; Kim, J.-J. *J. Chem. Phys.* **2003**, *118*, 2853.

MA052057H